

Three-mode opto-acoustic parametric interactions with coupled cavity

H. X. Miao* and C. Zhao, L. Ju, S. Gras, P. Barriga, Z. Y. Zhang and D. G. Blair

School of Physics, University of Western Australia, Western Australia 6009, Australia

(Dated: November 15, 2019)

Abstract

We theoretically analyze three-mode opto-acoustic parametric interactions in a coupled Fabry-Perot cavity. We show explicitly that extra degrees of freedom in the coupled cavity allow the exploration of both parametric instability and cooling regimes with high parametric gain in single table top experiment. This work can motivate experimental realizations of three-mode parametric instability, which can help us better model and understand possible parametric instabilities in next-generation gravitational-wave detectors. In addition, we show that the same system can be implemented to realize resolved-sideband acoustic mode cooling.

arXiv:0802.3534v3 [physics.optics] 6 Jul 2008

*Electronic address: miaoh01@student.uwa.edu.au

I. INTRODUCTION

Parametric interactions have wide applications and arouse great interests in various fields of physics, from high-sensitivity transducers to low-noise amplifiers and optical parametric oscillators. Two-mode parametric interaction have been used to cool acoustic modes of macroscopic mechanical oscillators. In Ref. [1], the authors used a microwave parametric transducer to cool the normal mode of a 1.5 tonne Nb bar down to 5mK. The same principle has also been applied to nanomechanical devices. In Ref. [2], a superconducting single-electron transistor (SSET) was coupled with a mechanical resonator to cool a very high frequency acoustic mode. More recently, using acoustic resonators coupled to optical cavity, various table top experiments have demonstrated significant cooling of the acoustic mode of the mechanical oscillators [3, 4, 5, 6, 7, 8, 9, 10, 11, 12, 13]. These experiments show great potential of achieving quantum ground state of macroscopic mechanical oscillators.

Three-mode opto-acoustic parametric interactions were first investigated by Braginsky et al. [14, 15] in the context of long Fabry-Perot cavities for interferometric gravitational-wave detectors. It was shown that three-mode interactions led to a risk of parametric instability (PI) in which the amplitude of an acoustic mode in a mirror could grow exponentially, thus undermining the sensitive operation of the detector. Parametric instability is governed by the same principles as mode cooling, except that the parametric gain has the opposite sign. The cause of the instability is the radiation pressure mediated nonlinear coupling between optical modes and acoustic modes in high optical power cavities. This can occur if two conditions are satisfied. First, the shape of high order cavity mode, hereafter denoted by TEM_{mn} must have a substantial overlap with the shape of the acoustic mode. Second, the mode gap between TEM_{mn} and TEM_{00} should be equal to the acoustic mode frequency up to an error of linewidth of the cavity mode. Many further theoretical studies have followed up after this pioneering work. Zhao et al. [16] extended their analysis and took into account the 3D acoustic mode structure of the mirrors and the optical cavity mode shapes. Ju et al. [17] further considered the overall contributions from multiple optical modes, showing that multiple interactions increase the risk of instability. Gurkovsky et al. [18] analyzed PI in the signal recycled (SR) interferometer, showing that the chance of PI was reduced due to the narrow linewidth of SR interferometer. Additionally, many ideas have been proposed to prevent PI. These include changing the radius of curvature (RoC) of the mirror [16], the

use of an optical spring tranquilizer [19] and the ring damper [20]. In the light of the above predictions, it is important to develop experimental techniques for their investigations. In recent progress, the University of Western Australia group used a capacitor to excite the acoustic mode and made the demonstration of the three-mode interactions with an 80m long Fabry-Perot cavity in the High Optical Power Facility (HOPF) at Gingin [21]. In the experiment, they used a compensation plate as a thermal lens to tune the effective (RoC) of the mirror so as to change the Gouy phase, or equivalently the mode gap. This enables the resonant condition mentioned to be satisfied. This experiment confirmed the principle of the three-mode interactions, but due to the small overlap and low optical power, it had not yet observed self-sustained parametric instability or cooling. In this paper, we propose another method of tuning the Gouy phase, which was first introduced by Mueller [22] as a means of designing a stable recycling cavity for the next-generation gravitational-wave detectors. Using an additional mirror and lens to form a coupled cavity, one can achieve any desired Gouy phase shift. This enables easy mode matching by adjusting the relative position of the mirrors. In the next sections, we will demonstrate explicitly that a small scale apparatus can be constructed that allows observation of three-mode interactions with high gain in table top experiments. This can be applied in general as a design concept for opto-acoustic parametric amplifiers and specifically to the resolved-sideband cooling [23, 24] of acoustic modes.

This paper is organized as follows: In Sec. II we will review the theory of three-mode opto-acoustic interactions. In Sec. III we discuss how to use the coupled cavity to explore the three-mode interactions in table top experiments. Finally, we summarize our results in Sec IV. The main notations used in this paper are listed in Table. I.

TABLE I: Main notations used in this paper.

Quantity	Value for Estimates	Descriptions
\hbar	1.054×10^{-34} J s	Planck constant
c	3×10^8 m/s	Speed of light
\mathcal{R}	$\pm 1 \sim \pm 10^5$	Parametric gain
m	~ 1 mg	Mass of mechanical oscillator
ω_m	$2\pi \times 10^6$ s ⁻¹	Eigenfrequency of the oscillator
Q_m	10^6	Quality factor of the oscillator
γ_m	$\omega_m/2Q$	Half linewidth of the mechanical resonance
ω_0	1.77×10^{15} s ⁻¹	Optical pumping frequency
ω_1	$\sim \omega_0$	Frequency of the high order mode
I_0		Input optical power
I_c	100 mW	Intracavity optical power
γ_s, γ_a	$2\pi \times 10^4 \sim 2\pi \times 10^5$ s ⁻¹	Linewidth of the optical resonance
Q_s, Q_a	$\Omega_{s(a)}/2\gamma_{s(a)}$	Quality factor of the optical resonance
Λ_a, Λ_s	~ 1	Overlapping factor between optical and acoustic mode
$\Delta\omega_{s(a)}$	~ 0	Frequency detuning
L_{01}	~ 30 cm	Length of the sub-cavity
L_{12}	~ 10 cm	Length of the main cavity
$\delta\phi_{01,12}$		Round-trip phase shift
Φ_g		Gouy phase
$R_{0,1,2}$		Radius of curvature of the mirrors
$r_{0,1,2}$		Amplitude reflectivity
$t_{0,1,2}$		Amplitude transmissivity
$A_{0,1,2}$	500 ppm	Optical loss

II. REVIEW OF THREE-MODE OPTO-ACOUSTIC PARAMETRIC INTERACTION THEORY

For coherence of this article, we will briefly review the theory of three-mode opto-acoustic parametric interactions in this section. The three-mode interactions can be understood in both quantum and classical pictures. In the former picture, we can treat the Fabry-Perot cavity as a multi-level quantum system occupied by photons, while the mechanical oscillator (end mirror) consists of phonon (acoustic) modes in different energy eigenstates. For simplicity, we only consider one phonon mode, which also represents most realistic experimental situations. Initially, the photons stay in one eigenstate (the TEM₀₀ mode). Resonant ampli-

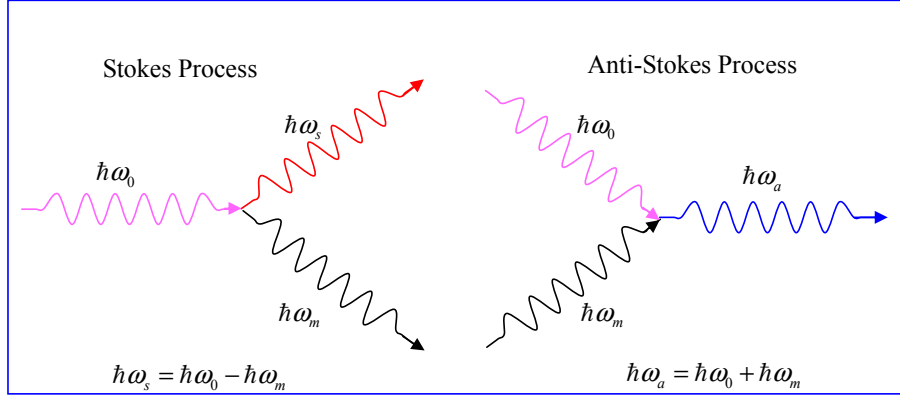


FIG. 1: Parametric interactions between photons and phonons. In the Stokes process, a photon is down converted into a phonon with lower energy and at the same time one phonon is created. This process will transfer energy from the optical field into mechanical degree of freedom, thus amplifying the acoustic mode. In the Anti-Stokes process, the photon is scattered into a higher-frequency photon, accompanied by annihilation of one phonon. In this process, the mechanical oscillation is damped. Classically, these two simply correspond to the processes where the light is modulated by the mechanical oscillation into two sidebands at frequencies $\omega_0 \pm \omega_m$.

fication occurs when the photons are scattered by the phonons into another eigenstate (the TEM_{mn} mode) of the cavity. The phonons can absorb energy from the photons (conventionally known as a Stokes process in Raman scattering) which causes instability. Alternatively, they can release energy into the photon field (Anti-Stokes process) which reduces the phonon occupation number, and is often described as cooling. We show both processes schematically in Fig.(1). In classical picture [14], the pumping frequency ω_0 is modulated into two sidebands due to the mechanical oscillation. The lower sideband corresponds to the Stokes mode with frequency $\omega_s = \omega_0 - \omega_m$; The upper sideband is the Anti-Stokes mode $\omega_a = \omega_0 + \omega_m$. If the sideband frequency matches the frequency of TEM_{mn} ω_1 , higher-order optical mode will be excited. In turn, these two resonant optical fields TEM_{mn} and TEM_{00} will exert an radiation pressure at the beating frequency $|\omega_1 - \omega_0| = \omega_m$. Depending on the phase, this force will either amplify or damp the motion of the oscillator. To achieve good coupling, it requires a substantial spatial overlap the acoustic mode and the TEM_{mn} mode.

To quantify the interactions, we follow the formalism given by Braginsky et. al [14]. In the paper, the authors introduced parameter gain \mathcal{R} to evaluate the strength of the three-mode

interactions, which is defined as,

$$\mathcal{R} = \frac{4I_c Q_m}{mcL\omega_m^2} \left[\frac{Q_s \Lambda_s}{1 + (\Delta\omega_s/\gamma_s)^2} - \frac{Q_a \Lambda_a}{1 + (\Delta\omega_a/\gamma_a)^2} \right]. \quad (1)$$

Here subscript s denotes Stokes mode and a represents Anti-Stokes mode. The detunings $\Delta\omega_{s(a)} \equiv |\omega_{s(a)} - \omega_1|$. The length L of the main cavity is chosen to be around ~ 10 cm for table top experiment. Overlapping factor $\Lambda_{a(s)}$ is given by,

$$\Lambda_{a(s)} = \frac{V \left(\int f_0(\vec{r}_\perp) f_{a(s)}(\vec{r}_\perp) u_z d\vec{r}_\perp \right)^2}{\int |f_0|^2 d\vec{r}_\perp \int |f_{a(s)}|^2 d\vec{r}_\perp \int |\vec{u}|^2 dV}, \quad (2)$$

where $f_{0,a,s}$ is the spatial distribution of the optical modes; u_z is the component of \vec{u} normal to the mirror surface; The integrals $\int d\vec{r}_\perp$ and $\int dV$ correspond to integration over mirror surface and volume V respectively. For simplicity, we assume that $\Lambda_{s(a)} \sim 1$, which can be achieved in real experiment. For the tuned case, \mathcal{R} can be greatly simplified as,

$$\mathcal{R} = \pm \frac{4I_c Q_m Q_{s(a)}}{mcL\omega_m^2}, \quad (3)$$

with $+$ for the Stokes process and $-$ for the Anti-Stokes process. The resulting linewidth or decay rate of the acoustic mode γ'_m is given by

$$\gamma'_m = \frac{1}{2} \left[(\gamma_{s(a)} + \gamma_m) - \sqrt{(\gamma_{s(a)} - \gamma_m)^2 + 4\mathcal{R}\gamma_{s(a)}\gamma_m} \right]. \quad (4)$$

Since usually the linewidth of the optical cavity $\gamma_{a(s)}$ is much larger than the mechanical linewidth γ_m , then

$$\gamma'_m \approx \gamma_m - \mathcal{R}\gamma_m. \quad (5)$$

When $\mathcal{R} = 0$, we have the trivial case $\gamma'_m = \gamma_m$. For the Stokes process $\mathcal{R} > 0$ (positive gain), the decay rate of the acoustic mode becomes smaller, which also means the mechanical oscillation will be amplified. If $\mathcal{R} > 1$, the real part of the eigenvalue is positive which means that the mode is unstable and PI will occur. For the Anti-Stokes process $\mathcal{R} < 0$ (negative gain), we cool the acoustic mode, and the maximum damping rate can be achieved when the square root in Eq.(4) vanishes, namely

$$\mathcal{R} \simeq -\frac{1}{4} \frac{\gamma_{a(s)}}{\gamma_m}, \quad (6)$$

which gives the upper limit of the cooling

$$\gamma'_m = \frac{1}{2} (\gamma_{a(s)} + \gamma_m) \sim \frac{1}{2} \gamma_{a(s)}. \quad (7)$$

Therefore the upper limit of cooling is set by the linewidth of the TEM_{mn} mode which can be at least 10^5 times larger than γ_m , which means that we can reduce the thermal occupation number of the acoustic mode by a factor of 10^5 if technical noise can be neglected.

III. THREE-MODE INTERACTIONS WITH COUPLED CAVITY

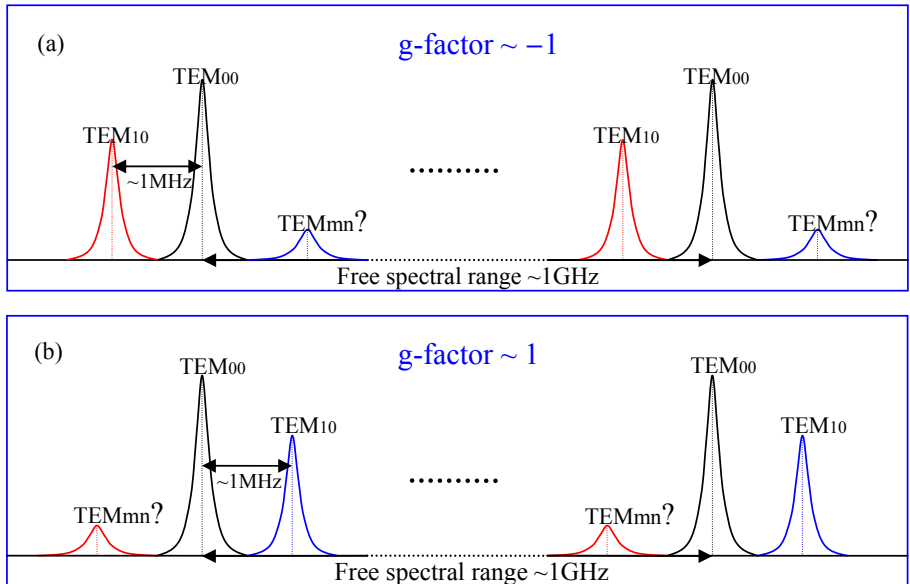


FIG. 2: The optical modes of single Fabry-Perot cavity with length ~ 10 cm. The panel (a) shows the mode distribution for the near-concentric cavity with g -factor ~ -1 , which enables one to observe PI, while panel (b) is the near-planar case with g -factor ~ 1 , which can be used to explore the regime of parametric cooling. In both cases, there are no symmetric modes on the opposite side of the TEM₀₀ mode because the higher order mode TEM _{mn} marked with “?” are highly lossy due to diffraction losses. This is preferred for experimental realizations of three-mode interactions because we know from Eq.(1) that any symmetric mode on the opposite side of the TEM₀₀ mode will reduce the absolute value of parametric gain. However, both cavities are marginally stable and very susceptible to misalignment.

In this section, we will discuss how to explore three-mode interactions using a coupled cavity. To make our analysis close to realistic experiments, we will consider a torsional acoustic mode ~ 1 MHz interacting with the TEM₁₀ and TEM₀₀ modes. The configuration is chosen because MHz can be easily achieved in mm-scale structure and the torsional mode has a large spatial overlap with the optical TEM₁₀ mode.

To begin with, we consider single Fabry-Perot cavity to see why we need a coupled cavity. The free spectral range of single cavity with length ~ 10 cm is approximately 1GHz. Therefore, as shown in Fig.(2), one has to build either a near-planar or near-concentric cavity to obtain desired mode gap between TEM₁₀ and TEM₀₀ around 1MHz. For both

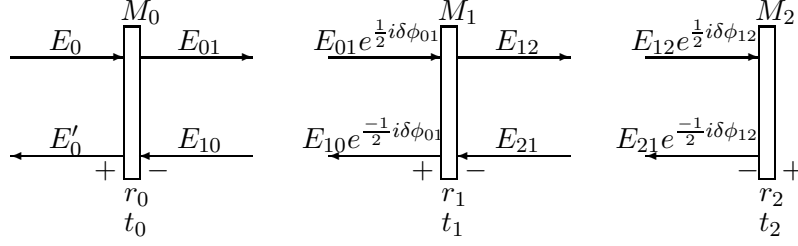


FIG. 3: The fields of the coupled cavity. Here $\delta\phi_{01,12}$ are the round-trip phase shift of light in the sub-cavity (formed by M_0 and M_1) and main cavity (formed by M_1 and M_2) respectively. We use the convention that mirror has minus reflectivity on the side with coating layer.

cases, the cavity is marginally stable and susceptible to misalignment. It is also difficult to access both instability and cooling regimes in single experimental setup.

A coupled Fabry-Perot cavity can solve these problems. We will see later that on the one hand, the resulting cavity is stable and on the other hand, we can easily tune between instability and cooling regimes. The coupled cavity is showed schematically in Fig.(3). It is similar to the configuration of power or signal-recycled Michelson type interferometers [25, 26] when one considers either common mode or differential mode. The dynamics of the fields in this system can be easily obtained as given by Rakhmanov [27]. Here we follow his approach and treat sub-cavity as an effective mirror with frequency and mode-dependent transmissivity and reflectivity. Specifically, effective transmissivity t_{01} is given by

$$t_{01} \equiv \frac{E_{12}}{E_0} = \frac{t_0 t_1}{1 + r_0 r_1 e^{i\delta\phi_{01}}}, \quad (8)$$

and effective reflectivity r_{10} is given by

$$r_{10} \equiv \frac{E_{12}}{E_{21}} = -r_1 - \frac{t_1^2 r_0 e^{i\delta\phi_{01}}}{1 + r_0 r_1 e^{i\delta\phi_{01}}}. \quad (9)$$

Then E_{12} inside the main cavity can be written as

$$E_{12} = \frac{E_0 t_{01}}{1 + r_{10} r_2 e^{i\delta\phi_{12}}} = \frac{E_0 t_{01}}{1 - |r_{10}| r_2 e^{i[\arg(r_{10}) + \delta\phi_{12} + \pi]}}. \quad (10)$$

The resonance occurs when phase factor in Eq.(10) is equal to $2n\pi$, which depends critically upon the phase angle of the effective reflectivity, namely $\arg(r_{10})$. Specifically, when the

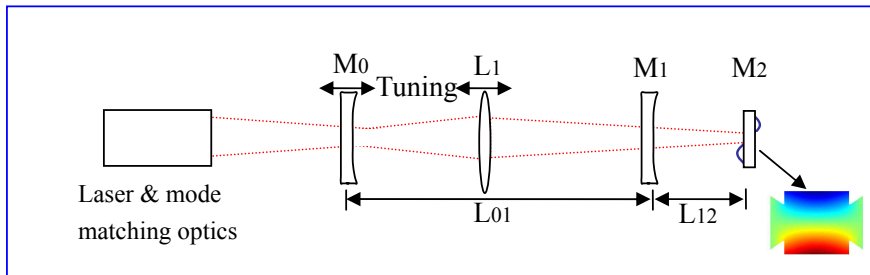


FIG. 4: The optical layout for the table top experiment. The locations of the mirror M_0 and the lens L_1 define the high order mode frequency. Mirror M_2 is the interacting mirror, consist of the 1 MHz mini torsional oscillator. If the losses in L_1 were an issue, it could easily be replaced by a concave mirror. The system analyzed here uses an acoustic mode interacting with the TEM_{10} mode and the TEM_{00} mode. The TEM_{10} mode has a good spatial overlap with the torsional acoustic mode.

TEM_{00} mode resonates inside the main cavity, which requires that $\delta\phi_{01}^{TEM_{00}} = \delta\phi_{12}^{TEM_{00}} = 2n\pi$, phase shift of the TEM_{10} mode $\delta\phi_{ij}^{TEM_{10}}$ is

$$\delta\phi_{ij}^{TEM_{10}} = \frac{2L_{ij}}{c}\Delta\omega - 2\Phi_g^{ij} + 2n'\pi, \quad ij = 01, 12, \quad (11)$$

where $\Delta\omega \equiv \omega_1 - \omega_0$ is the mode gap between TEM_{10} and TEM_{00} ; Φ_g is the Gouy phase and n, n' are integer numbers. In order to satisfy the conditions for three-mode interactions, we need to adjust $\delta\phi_{01}^{TEM_{10}}$, which changes $\arg(r_{10})$, such that $\Delta\omega = \pm\omega_m$. To achieve this, one obvious way is to change the length of sub-cavity L_{01} , but this turns out to be impractical due to small tuning range. An alternative and more practical way, as shown in Fig.(4), is to add another lens or concave mirror inside the sub-cavity to tune the Gouy phase Φ_g^{01} . This approach is similar to proposed stable recycling cavity designs for next-generation gravitational-wave detectors [22]. With additional lens, the Gaussian beam get focused inside the sub-cavity. Since Gouy phase changes almost from $-\frac{\pi}{2}$ to $\frac{\pi}{2}$ within one Rayleigh range around the waist, one can easily obtain desired $\delta\phi_{01}^{TEM_{10}}$ simply by adjusting the position of M_0 near the waist. This might lead to problems with power density due to the small waist size, but for the table top experiment we consider here, the power density is quite low.

The corresponding Φ_g^{01} when a lens is added can be derived straightforwardly using ray

transfer relation for the Gaussian beam, which is given by

$$q' = \frac{fq}{f - q}. \quad (12)$$

Here f is focal length of L_1 ; $q^{(l)} \equiv z^{(l)} + iz_R^{(l)}$; z is the displacement relative to the waist; z_R is Rayleigh range and superscript $'$ denotes the quantity after the lens. This dictates

$$z' = \frac{f(zf - z^2 - z_R^2)}{(f - z)^2 + z_R^2}, \quad (13)$$

$$z'_R = \frac{z_R f^2}{(f - z)^2 + z_R^2}. \quad (14)$$

The resulting Gouy phase at any point is given by

$$\Phi_g(z) = \begin{cases} \arctan(z/z_R), & z < z_L \\ \arctan[(z - z_L + z'_L)/z'_R] + \arctan(z_L/z_R) - \arctan(z'_L/z'_R), & z \geq z_L \end{cases} \quad (15)$$

where $z_L^{(l)}$ is the position of L_1 relative to the waist. Gouy phase Φ_g^{01} is given by the phase difference between phase front at M_0 and the one at M_1 , namely

$$\Phi_g^{01} = \Phi_g(z_{M_0}) - \Phi_g(z_{M_1}), \quad (16)$$

where z_{M_0} and z_{M_1} are the positions of M_0 and M_1 relative to the waist respectively. Therefore, by adjusting the positions of M_0 and L_1 as shown in Fig.(4), we can continuously tune Φ_g^{01} such that $\Delta\omega = \omega_m$.

Eq.(8)~Eq.(16) provide the design tools of the coupled cavity for three-mode interactions. To realize the experiment, we first need to design the main cavity and specify L_{12} , ω_m , the RoCs of the mirrors M_0, M_1, M_2 and the focal length of L_1 . Then from Eq.(10) and Eq.(11), we can find required $\arg(r_{01})$ to obtain the right mode gap between TEM_{10} and TEM_{00} . This will provide one constraint to the system. Combining with the constraint from the requirement of mode matching to M_0 , we can fix these two degrees of freedom of the system, namely the positions of M_0 and L_1 . To demonstrate the principle explicitly, we present a

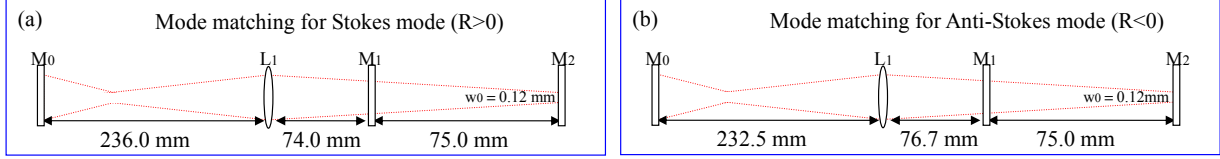


FIG. 5: The mode matching for the positive gain and negative gain by adjusting the relative position of M_0 and L_1 . Only small adjustment is needed to tune from one case to another.

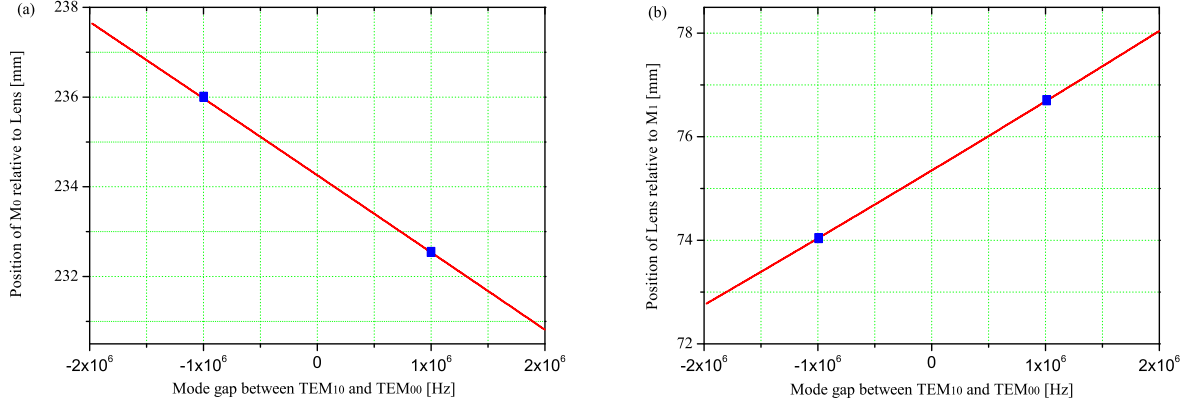


FIG. 6: The panels (a) and (b) show the mode gap between TEM_{10} and TEM_{00} as a function of position of M_0 relative to L_1 and position of L_1 relative to M_1 respectively. The dots in both figures are the situations considered in Fig.(5). Clearly, we can tune between the instability and cooling regimes continuously.

solution that is close to a realistic experimental setup. We assume the following,

$$L_{12} = 75 \text{ mm} \quad \omega_m = 1\text{MHz} \quad f = 100 \text{ mm}$$

$$R_0 = 500 \text{ mm} \quad r_0 = \sqrt{0.999} \quad A_0 = 500 \text{ ppm}$$

$$R_1 = 100 \text{ mm} \quad r_1 = \sqrt{0.9} \quad A_1 = 500 \text{ ppm}$$

$$R_2 = \infty \text{ mm} \quad r_2 = \sqrt{0.9995} \quad A_2 = 500 \text{ ppm}$$

Here $R_i (i = 0, 1, 2)$ are RoCs of corresponding mirror; r_i denotes amplitude reflectivity; t_i is amplitude transmissivity and A_i is optical loss which satisfy $r_i^2 + t_i^2 + A_i = 1$ ($i = 0, 1, 2$).

The results of mode matching for both positive (instability) and negative gain (cooling) configurations are shown in Fig.(5). In Fig.(6), we show dependence of mode gap between TEM_{10} and TEM_{00} on position of M_0 relative to L_1 and position of L_1 relative to M_1 . In this

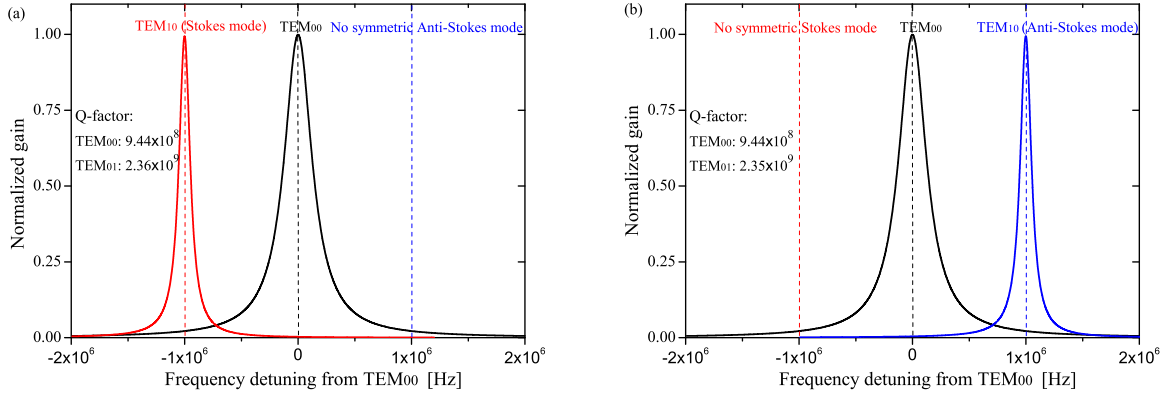


FIG. 7: The normalized gain of the TEM_{00} mode and the TEM_{10} mode in the positive and negative gain configurations. The mode gap is equal to $\omega_m \sim 1\text{MHz}$, which fulfils the resonant condition for the three-mode opto-acoustic interactions. The quality factor of each mode is shown. Here we simply assume that the size of the mirrors is infinite so the quality factor of the TEM_{10} mode is not influenced by diffraction loss but only the optical losses such as absorption. This assumption is reasonable when the mode number is small. For the given parameter values, we can see that it is in the good cavity regime where $\omega_m/\gamma_a < 1$. This can be implemented in the resolved-sideband cooling. (a) The TEM_{10} mode is 1 MHz below the TEM_{00} mode; (b)The TEM_{10} mode is 1 MHz above the TEM_{00} mode.

particular case, the functional dependence is almost linear and the slope is $1.5 \sim 2\text{mm/MHz}$ for both panels. This indicates that to tune within the cavity linewidth $\sim 0.1\text{ MHz}$, it requires the mirror position to be adjusted within several $100\mu\text{m}$, which can be achieved easily. Therefore, we can continuously tune between instability and cooling regimes. Fig.(7) shows the resulting resonance curves for both the positive and negative gain cases with corresponding mode matching shown in Fig.(5). In both cases, the mode gap between TEM_{10} and TEM_{00} is equal to $\omega_m \sim 1\text{MHz}$. More importantly, there is no corresponding symmetric mode on the opposite side of the TEM_{00} mode, whose presence could contribute parametric gain with opposite sign, thereby suppressing the overall parametric effects. This means that coupled cavity can explore three-mode interactions very efficiently. The absolute value of parametric gain \mathcal{R} will be larger than 1 if we assume that intracavity power I_c is 100 mW, $Q_m = 10^6$, mass of the oscillator $m = 1\text{ mg}$, wavelength of the laser is 1064 nm. Since the cavity is in good cavity regime where cavity linewidth is much smaller than mechanical

frequency [23], this configuration can also be applied in resolved-sideband cooling of the acoustic mode, which makes coupled cavity system less susceptible to quantum noise in the cooling regime. Although quantum noise analysis given by Refs. [23, 24, 28] only discussed two-mode system, the result can be directly applied to this three-mode system. Because we can view the TEM₀₀ mode as a pumping field, and only the asymmetry spectrum of the Anti-Stokes or Stokes modes contribute to the cooling and the quantum noise. This can be justified by writing down the Hamiltonian of this three-mode opto-acoustic system,

$$\hat{H} = \frac{\hat{p}^2}{2m} + \frac{1}{2}m\omega_m^2\hat{x}^2 + \hbar\omega_0\hat{a}^\dagger\hat{a} + \hbar\omega_1\hat{b}^\dagger\hat{b} + \hbar G_0\hat{x} \left(\hat{a}^\dagger\hat{b} + \hat{b}^\dagger\hat{a} \right) + i\hbar E \left(\hat{a}^\dagger e^{-i\omega_0 t} - \hat{a} e^{i\omega_0 t} \right), \quad (17)$$

with coupling constant $G_0 \equiv \omega_0/L$ and $E \equiv \sqrt{2\gamma I_0/\hbar\omega_0}$. Here first two terms describe the acoustic mode where \hat{x} is the displacement and \hat{p} is the momentum which satisfy commutation relation $[\hat{x}, \hat{p}] = i\hbar$; \hat{a} and \hat{b} is the lowering operator of TEM₀₀ and TEM₁₀ respectively; the fifth term quantifies the interactions between optical modes and acoustic mode; the last term is the driving term. It is straightforward to show that this Hamiltonian will give the same equations of motion as in Ref. [14] if mechanical loss, optical loss and overlapping factor are properly included. Since only TEM₀₀ is pumped with laser, the interaction term can be linearized as

$$\hbar G_0\hat{x} \left(\bar{a}^*\hat{b} + \bar{a}\hat{b}^\dagger \right), \quad (18)$$

which is the same interaction term as in Ref. [23, 28] after linearizing. Therefore, the three-mode Hamiltonian can be mapped into an effective two-mode Hamiltonian by replacing \hat{a} with its steady state value \bar{a} . All the conclusions reached in the two-mode case also satisfy here. The only difference is that our pumping field TEM₀₀ is also on resonance. Therefore, we can achieve resolved-sideband limit without compromising the high intra-cavity optical power. If technical noises can be sufficiently small, we can achieve quantum ground state of 1MHz oscillator starting from 4K when $\mathcal{R} \sim 10^5$, which corresponds to the case that $m = 0.1$ mg, $Q_m = 10^7$, $I_c = 10$ W and $Q_a = 10^{10}$.

IV. CONCLUSION

We have shown that small scale three-mode opto-acoustic parametric amplifiers (OAPA) based on the use of a coupled cavity can be designed that allow both three-mode parametric instability and acoustic mode cooling with high gain to be explored in single table top

experiment. This theoretical work can motivate new experimental investigations of three-mode parametric instability which may be an issue in the next-generation gravitational-wave detectors, helping in the development of better models, and in developing techniques for control. In the high negative gain regime, the same configuration enables high negative gain resolved side band cooling of acoustic modes. In future we intend to demonstrate the advantages of the OAPA for cooling, especially since the system should have reduced sensitivity to laser phase noise.

ACKNOWLEDGEMENTS

We thank all the participants attending the Parametric Instability Workshop held at the Australian International Gravitational Observatory (AIGO) site, especially Prof. Vyatchanin and Strigin for stimulating discussions and pointing out several errors in the manuscripts and giving precious advices on the improvement of the draft. H.X. thanks Prof. Yanbei Chen for his invitation to visit Albert-Einstein-Institut with the funding supported by Alexander von Humboldt Foundation's Sofja Kovalevskaja Programme. This research was supported by the Australian Research Council and the Department of Education, Science and Training and by the U.S. National Science Foundation. We thank the LIGO Scientific Collaboration International Advisory Committee of the Gingin High Optical Power Facility for their support.

-
- [1] D. G. Blair, E. N. Ivanov, M. E. Tobar, P. J. Turner, F. van Kann & I.S. Heng. *Phys. Rev. Lett.* **74**, 1908 (1995);
 - [2] A. Naik, O. Buu, M. D. LaHaye, A. D. Armour, A. A. Clerk, M. P. Blencowe and K. C. Schwab. *Nature* **443**, 14 (2006);
 - [3] S. Gigan, H. R. Böhm, M. Paternostro, F. Blaser, G. Langer, J. B. Hertzberg, K. C. Schwab, D. Bäuerle, M. Aspelmeyer & A. Zeilinger. *Nature* **444**, 67 (2006);
 - [4] O. Arcizet, P. F. Cohandon, T. Briant, M. Pinard & A. Heidmann. *Nature* **444**, 71 (2006);
 - [5] Dustin Kleckner & Dirk Bouwmeester. *Nature* **444**, 75 (2006);
 - [6] A. Schliesser, P. DelHaye, N. Nooshi, K. J. Vahala, and T. J. Kippenberg, *Phys. Rev. Lett.* **97**, 243905 (2006);

- [7] T. Corbitt, Y. Chen, E. Innerhofer, H. Muller-Ebhardt, D. Ottaway, H. Rehbein, D. Sigg, S. Whitcomb, C. Wipf & N. Mavalvala. Phys. Rev. Lett. **98**, 150802 (2007);
- [8] T. Corbitt, C. Wipf, T. Bodiya, D. Ottaway, D. Sigg, N. Smith, S. Whitcomb, and N. Mavalvala, Phys. Rev. Lett. **99**, 160801 (2007);
- [9] A. Schliesser, R. Riviere, G. Anetsberger, O. Arcizet, T. J. Kippenberg. arXiv: 0709.4036v1 [quant-ph] (2007);
- [10] M. Poggio, C. L. Degen, H. J. Mamin, and D. Rugar. Phys. Rev. Lett. **99**, 017201 (2007);
- [11] J. D. Thompson, B. M. Zwickl, A. M. Jayich, Florian Marquardt, S. M. Girvin and J. G. E. Harris. arXiv:0707.1724v2 (2007);
- [12] C. M. Mow-Lowry, A. J. Mullavey, S. Goßler, M. B. Gray and D. E. McClelland. Phys. Rev. Lett. **100**, 010801 (2008);
- [13] S.W. Schediwy et al. (to be appeared in Phys. Rev. A);
- [14] V. B. Braginsky, S. E. Strigin & S. P. Vyatchanin. Phys. Lett. A **287**, 331 (2001);
- [15] V. B. Braginsky, S. E. Strigin & S. P. Vyatchanin. Phys. Lett. A **305**, 111 (2002);
- [16] C. Zhao, L. Ju, J. Degallaix, S. Gras & D. G. Blair, Phys. Rev. Lett. **94**, 121102 (2005);
- [17] L. Ju, S. Gras, C. Zhao, J. Degallaix & D. G. Blair, Phys. Lett. A **354**, 360 (2006);
- [18] A.G. Gurkovsky, S.E. Strigin, S.P. Vyatchanin. Phys. Lett. A **362**, 91 (2007);
- [19] V. B. Braginsky & S. P. Vyatchanin. Phys. Lett. A **293**, 228 (2002);
- [20] S. Gras, D.G. Blair, L. Ju, *Test mass ring dampers with minimum thermal noise*, preprint (2006);
- [21] C. Zhao et.al, *Observation of Three Mode Parametric Interactions in Long Optical Cavities* submitted to Phys. Rev. A ;
- [22] Guido Mueller. LIGO document: G070441-00-R;
- [23] Florian Marquardt, Joe P. Chen, A. A. Clerk, and S. M. Girvin. Phys. Rev. Lett. **99**, 093902 (2007);
- [24] I. Wilson-Rae, N. Nooshi, W. Zwerger, and T. J. Kippenberg. Phys. Rev. Lett. **99**, 093901 (2007);
- [25] Brian J. Meers. Phys. Rev. D **38**, 8 (1988);
- [26] A.Buonanno, Y.Chen, Phys. Rev. D **64**, 042006 (2001);
- [27] Malik Rakhmanov. *Dynamics of Laser Interferometric Gravitational Wave Detectors* (2000) (PhD Thesis);

- [28] C. Genes, D. Vitali, P. Tombesi, S. Gigan and M. Aspelmeyer, Phys. Rev. A **77**, 033804 (2008).